Available online at www.sciencedirect.com
ScienceDirect
Physics Letters A 359 (2006) 640–646
PHYSICS LETTERS A
www.elsevier.com/locate/pla

Coherence and stochastic resonance in threshold crossing detectors with delayed feedback

Robert Morse [a,*], André Longtin [b]

[a] *MacKay Institute of Communication and Neuroscience, School of Life Sciences, Keele University, Keele ST5 5BG, United Kingdom*
[b] *Department of Physics, University of Ottawa, 150 Louis-Pasteur, Ottawa, K1N 6N5, Canada*

Received 8 May 2005; received in revised form 13 July 2006; accepted 14 July 2006

Available online 28 July 2006

Communicated by A.P. Fordy

Abstract

We consider the dynamical behavior of threshold systems driven by external periodic and stochastic signals and internal delayed feedback. Specifically, the effect of positive delayed feedback on the sensitivity of a threshold crossing detector (TCD) to periodic forcing embedded in noise is investigated. The system has an intrinsic ability to oscillate in the presence of positive feedback. We first show conditions under which such reverberatory behavior is enhanced by noise, which is a form of coherence resonance (CR) for this system. Further, for input signals that are subthreshold in the absence of feedback, the open-loop stochastic resonance (SR) characteristic can be sharply enhanced by positive delayed feedback. This enhancement is shown to depend on the stimulus period, and is maximal when this period is matched to an integer multiple of the delay. Reverberatory oscillations, which are particularly prominent after the offset of periodic forcing, are shown to be eliminated by a summing network of such TCDs with local delayed feedback. Theoretical analysis of the crossing rate dynamics qualitatively accounts for the existence of CR and the resonant behavior of the SR effect as a function of delay and forcing frequency.

1. Introduction

Feedback is an important concept in many areas of science, particularly in physics [1]. The temporal evolution of a system with delayed feedback is dependent not only on the current value of state variables but also on their past values. Delayed feedback occurs in many nonlinear systems such as optical resonators [2–4], chemical reactions [5], biological [6,7] and artificial [8] neural nets, and genetic and other physiological control systems [9,10]. The importance of delayed feedback has further been highlighted in chaos control [4,11], chaos communication [3], and anticipatory chaos control [12]. Memory effects due to feedback strongly affect the dynamics when the associated delays are commensurate with or longer than the time scales of the system without feedback.

Many such feedback systems, including excitable biological or optical systems, further involve sharp activation functions, or "thresholds", and are driven by noise [13] and one or more periodic inputs. The effect of noise on the switching properties of threshold systems has received much interest in the context of coherence resonance (CR) [15] and stochastic resonance (SR) [14,16–19]. In particular, there have been very recent studies of the enhancement by noise of the oscillations in a network of delayed-coupled oscillators [21] and in a bistable discrete-time stochastic map [22], of stochastic resonance in a non-Markovian system [23] and of control of noise-induced motion in relaxation oscillators using delayed feedback [24]. Recent studies have also highlighted the potential usefulness of *instantaneous* feedback on SR [25–27].

The novel synergistic effects of noise and *delayed* feedback on the synchronization of threshold elements to external input are the subject of our Letter. We focus on single and parallel arrays of threshold-crossing detectors (TCD). Each such thresholding element produces a stereotyped brief "spike" at the instants when a threshold level is exceeded, thus capturing in a simple manner the key nonlinear features of excitable systems, biological, optical or other. Our results apply however to

* Corresponding author.
E-mail address: r.p.morse@aston.ac.uk (R. Morse).

0375-9601/$ – see front matter
doi:10.1016/j.physleta.2006.07.014

a large class of noisy systems with delayed feedback and external forcing. We find that the interaction of an intrinsic mode due to delayed feedback with external forcing and noise leads to a strong amplification of subthreshold input when the input period matches the delay. Another way of describing this behavior is to say that the TCD acts as a strong frequency selector, i.e., it will tend to resonate with and thus amplify a narrow range of frequencies from a broadband input.

Our Letter is organized as follows. In Section 2, we present the model used to study threshold elements with noise, deterministic input and delayed feedback. Section 3 shows numerical results on the behavior of a single threshold system without feedback ("open-loop") and with feedback ("closed loop"), and in particular, on the behavior of the signal-to-noise ratio (SNR) as the input noise intensity is varied. This section includes behavior of the system before and after sinusoidal forcing, which reveals the presence of reverberating oscillations. Section 4 then focuses on eliminating these reverberatory oscillations which are enhanced by a harmonic input of a certain frequency and outlast its presence. This is done by considering arrays of TCD's, each with their individual feedback. An approximate analytical characterization of the reverberations and dependence of the SNR on input frequency and feedback delay follows in Section 5.

2. Model TCD with feedback

The TCD is a nonlinear system that generates a brief spike—which for our purposes will be a Dirac delta function—whenever its input crosses a fixed threshold. In our study, we will confine the spike generation to crossings in the positive direction only. Also, we will consider a TCD driven by lowpass-filtered zero-mean Gaussian white noise, a sinusoidal input, and pulses ("spikes") from the output of this same TCD at a previous time (Fig. 1(a)). This latter driving force is the delayed feedback. The strength of this feedback is set by the feedback gain G defined below. In open loop, an input signal $A\sin(2\pi f_0 t)$ is subthreshold if it is less than the TCD threshold Δ_0 (this threshold is measured with respect to zero) after going through the lowpass filter of time constant τ_2 in front of the TCD, i.e., when $A(1+2\pi f_0\tau_2)^{-1} < \Delta_0$. This will always be the case for the periodic forcing in our study.

This characterization of the external input as "subthreshold" also holds in closed loop. However, in closed loop, one must also consider whether an input in the form of a feedback spike is sub- or suprathreshold. If $G < 1$, this spike will not reach the TCD threshold: this is the *subthreshold feedback* situation. Alternately, $G > 1$ corresponds to the *suprathreshold feedback* situation. In this latter case, and in the absence of any external input noise, a feedback spike will generate a sequence of spikes roughly one delay apart. Noise may interrupt this process, or may produce new spikes. In contrast, for the subthreshold case, a spike can perpetuate itself via feedback only with the help of external noise. As in the suprathreshold case however, noise can also prevent a spike from generating future spikes.

On its own, a stochastic input will generate spikes at random times, namely, whenever the stochastic input crosses the threshold from below. If the external noise is Gaussian white noise, it is known that the mean time between such crossings is zero unless precautions are taken to properly lowpass filter this noise (see, e.g., [16]). Specifically, the spectral power density of the input fluctuations must decay at least as fast as ω^4, or else the threshold crossing rate is infinite (this is also true for $\tau_1 = \tau_2$—see [28]). For this reason, we used throughout our study a doubly filtered Gaussian white noise as the input noise to a TCD, as in [16]. On its own this noise is governed by

$$\frac{d^2y}{dt^2} + \left(\frac{1}{\tau_1} + \frac{1}{\tau_2}\right)\frac{dy}{dt} + \frac{y}{\tau_1\tau_2} = \frac{1}{\tau_1\tau_2}\xi(t) \tag{1}$$

where ξ is zero-mean Gaussian white noise satisfying $\xi(t)\xi(t') = 2D\delta(t-t')$. *In the following, we will refer to D as the noise intensity*. This governing equation is actually realized as part of the equations for the full model stated below (Eq. (3)). In the context of our study, it is not necessary to describe this noise as internal or external; it could account for synaptic noise at the input to a neuron, or quantum noise in a laser cavity. For simplicity, we set $\tau_1 = \tau_2 \equiv \tau$. In contrast to the external noise, the feedback delta-spikes are singly filtered. The rationale for this choice is simplicity, and also the similarity to a neuron spike arriving at a cell and being transformed into a synaptic response via a lowpass filter.

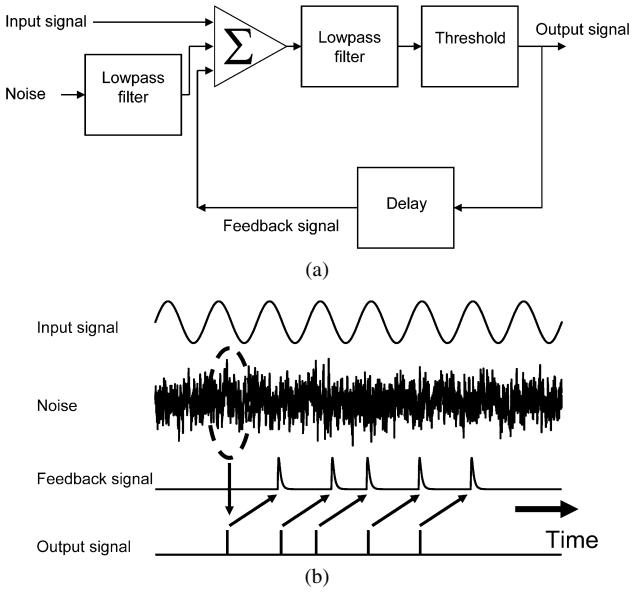

Fig. 1. (a) Schematic diagram for the threshold crossing detector with delayed feedback, driven by sinusoidal forcing and noise. (b) A time series of an input to the detector with, below it, the associated spikes produced by the detector. Feeding these spikes back to the input after a delay closes the feedback loop.

Mathematically, the model can be described as follows:

$$\tau_1\frac{dx}{dt} = -x(t) + \xi(t), \tag{2}$$

$$\tau_2\frac{dy}{dt} = -y(t) + x(t) + A\sin(2\pi f_0 t) + z_0\sum_n \delta(t - t_n - \tau_D), \tag{3}$$

where x is the output of the first (leftmost in Fig. 1) lowpass filter, y the output of the second lowpass filter (or input to the

TCD), f_0 the external forcing frequency, z_0 the strength of the feedback delta pulses, and t_n the nth firing time of the TCD. The feedback delay is denoted by τ_D. This system was integrated numerically with an Euler–Maruyama scheme. The dynamics are such that a feedback spike increments $y(t)$ by an amount z_0/τ_2, which allows to precisely define the feedback gain as $z_0/\tau_2 \equiv G$.

An exact theoretical analysis of the behavior of such a highly nonlinear stochastic system is problematic, in particular because of its non-Markovian property arising from the delay (see Section 5). Our study is thus based rather on numerical simulations and analytical approximations. For positive feedback, a feedback spike emitted τ_D seconds earlier pushes the input of the TCD towards, and perhaps even past threshold. Because the feedback is positive, this dynamical system has an inherent tendency towards instability, i.e. spontaneous fluctuations get amplified. For $G = 0$, i.e., the "open-loop" case, and without periodic forcing, the ensemble-averaged mean threshold-crossing rate ν due to the noise is predicted by Rice's formula [29] adapted to doubly-filtered Gaussian white noise [16]:

$$\nu_0 = \frac{4\pi \int_0^\infty f^2 S(f)\,df}{R(0)} \exp\left(-\frac{\Delta_0^2}{2R(0)}\right) \tag{4}$$

$$= \frac{1}{2\pi\tau} \exp\left(\frac{-\tau\Delta_0^2}{D}\right). \tag{5}$$

Here $R(0) = D/2\tau$ is the autocovariance at lag zero (i.e., the variance) of the doubly-filtered noise at the input of the TCD,

$$S(f) = 2D\left(1 + 4\pi^2 f^2 \tau^2\right)^{-2} \tag{6}$$

is its power spectral density, and Δ_0 is the threshold of the TCD measured with respect to zero. Fig. 2 illustrates the spectral properties of solutions of Eq. (3) with noise, periodic forcing and delayed feedback; the behavior is illustrated for two values of the noise intensity in both the *subthreshold* and *suprathreshold feedback* regimes. Multiple realizations of Eq. (3) were computed numerically. For each realization, a power spectrum of the spike train at the output of the TCD was calculated using the fast Fourier transform algorithm. In all our study, we averaged spectra over many realizations of the noise; however, we did not average over the phase of the input signal, which is fixed at the same value for all realizations. The spectra shown use a common frequency and power scale. In all cases, one sees a periodic structure in the spectra, at harmonics of the forcing frequency. The right panels show strong power at all harmonics, since the feedback is strong and reinforces existing spike patterns (i.e., they are more robust to the noise).

The signal in the rest of our study is a brief 1.6 second sine wave, and signal-to-noise ratios (SNR) are computed from firing data for 1.6 seconds before, during and after the signal presentation. One motivation for using such a signal is to understand detection of transient signals embedded in noise using delayed feedback; applications include neural prostheses [31]. We will see that, like many other systems, feedback sets up new intrinsic time scales that modify the intrinsic dynamics, and their ability to differentially respond to certain kinds of input.

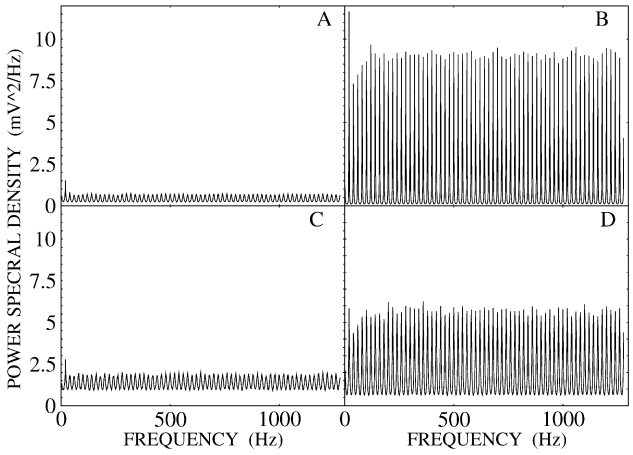

Fig. 2. Power spectra of the spike trains generated by the TCD output from Eq. (3). Specifically, for the subthreshold feedback regime ($G = 0.5$), we used (A) $D = 0.002$ and (C) $D = 0.01$. For the suprathreshold regime ($G = 1.5$), we used (B) $D = 0.002$ and (D) $D = 0.01$. Other parameters, held constant throughout our study, are: $\tau_D = 0.05$ s, $A = 0.5$, $f_0 = 20$ Hz, $\tau_1 = \tau_2 = 0.005$ s, and $\Delta_0 = 1.0$. With these parameters, the sinusoidal forcing is always below the TCD threshold in the absence of feedback, i.e., it is subthreshold. Each power spectrum was obtained by an ensemble average over spike trains from 400 realizations, each one lasting 1.6 seconds. Fast Fourier transforms were used on Hanning-windowed spike trains. The harmonic structure at all integer multiples of the fundamental (i.e., signal) frequency is clearly visible in all cases. Numerical integration was performed using the Euler–Maruyama technique with integration time step 2.5×10^{-5} s.

3. Resonances for a single TCD

We first consider the case where a single TCD is driven by noise and periodic input (subthreshold throughout our study) as well as feedback spikes. The ratio of the spectral power at the forcing frequency f_0 to the noise floor at f_0 was computed from the averaged spectrum. The resulting signal-to-noise ratio or SNR is plotted as a function of the noise intensity D in Fig. 3 for open-loop and closed loop conditions. For open-loop ($G = 0$), the SNR exhibits a unimodal curve, i.e., stochastic resonance (SR). This is consistent with results from previous work on SR in nondynamical threshold crossing systems [16,17,19] and leaky integrate-and-fire models of excitability [18,30].

In the open-loop case, the SNR differs from 1 only when the stimulus is on; results for SNR before and after the periodic stimulus are thus not shown. However, this is not the case in closed-loop. Fig. 3 shows the SNR versus D for $G = 0.5$, for a delay τ_D equal to the signal period $1/f_0$. The SNR was computed for two-second realizations before, during and after the sinusoidal forcing was on. We first note that the SNR-vs.-D curve during the signal is sharper in closed loop than in open loop. This attests to a stronger resonance in the closed loop system.

Further, in contrast with the open-loop case, the SNR-vs.-D curves before and after the signal have a similar shape to the one during the signal, but with a smaller amplitude (smaller in fact than for the open loop case during the signal). The noise in fact increases the strength of this intrinsic oscillation in this regime, which is a form of coherence resonance (CR) for this feedback system [15]. This is a consequence of reverberation

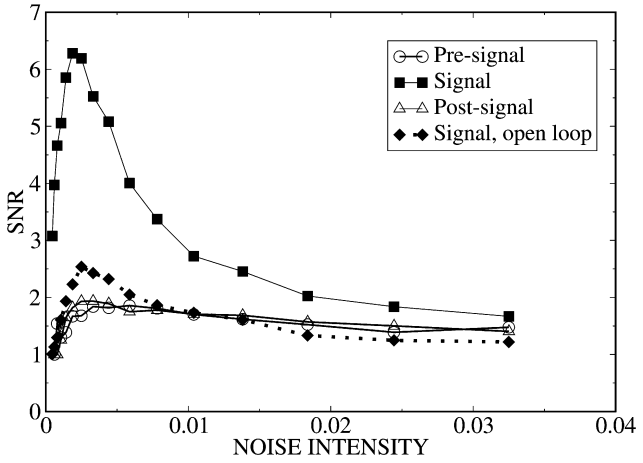

Fig. 3. Signal-to-noise ratio (SNR) versus external noise intensity D for the *subthreshold feedback regime* with $G = 0.5$ for a single TCD with feedback. The SNR is measured on the spike train from a single detector with a delay $\tau_D = 0.05$ ms in the subthreshold feedback regime ($G = 0.5$). Data are shown for three cases: the pre-signal case (1.6 seconds prior to sinusoidal forcing); the signal case (1.6 seconds of sinusoidal forcing at $f = 20$ Hz), and the post-signal case (1.6 seconds following the signal). Also plotted are the SNR data for the open-loop case $G = 0$. The SNR-vs.-D curve is more narrowly peaked in the feedback situation, i.e. the stochastic resonance is sharper. The pre- and post-signal cases also show resonances, which is a form of coherence resonance for this system. Each power spectral density was computed from an average over 2000 realizations of 1.6 seconds each. The signal component S is given by the power at 20 Hz, and the noise N was estimated by averaging the spectral powers at 10 and 30 Hz. The SNR is given by S/N. The uncertainty in the SNR is on the order of the symbol size used to plot the data.

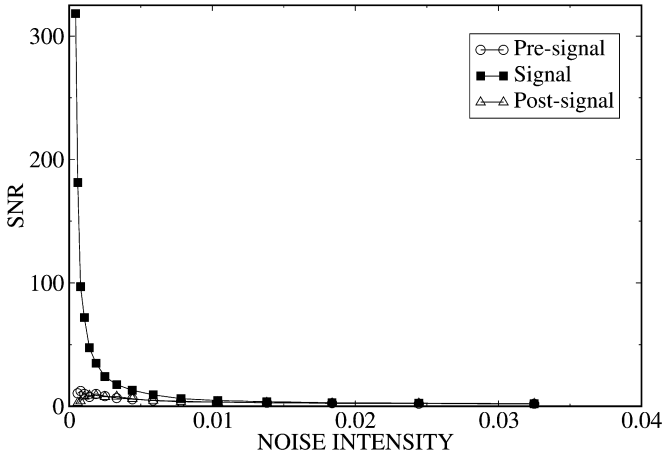

Fig. 4. SNR versus external noise intensity D as in Fig. 3, but for the *perithreshold feedback regime* $G = 1.0$.

caused by positive feedback: any spike generated by the noise will reduce the distance to threshold in the TCD after a delay.

In fact, the feedback alone can, with sufficient gain as in Fig. 4 ($G = 1.0$) and Fig. 5 ($G = 1.5$), act as a suprathreshold forcing, even though the first spikes were generated by noise and the periodic signal is subthreshold. One spike can statistically pertuate itself and generate new spikes over many successive delay periods; the noise will eventually suppress some or all of these spikes, and create new forward "avalanches" of spikes. This reverberatory activity is due to an intrinsic instability of the autonomous system (see below). The strength of

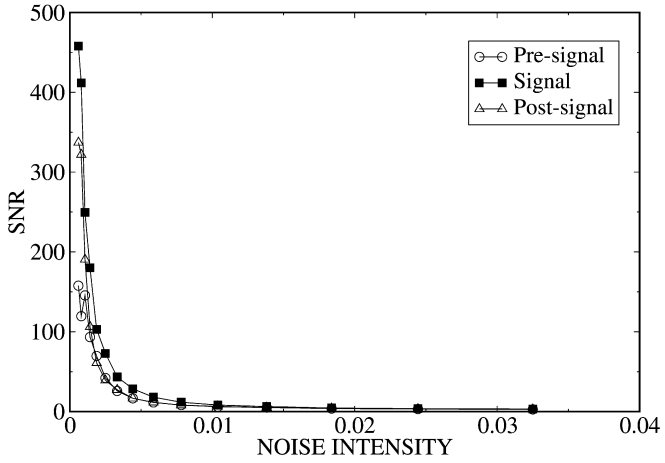

Fig. 5. SNR versus external noise intensity D as in Fig. 3, but for the *suprathreshold feedback regime* with $G = 1.5$.

the SNR simply increases with the feedback gain, and for the gains in Figs. 4 and 5, the SNR-vs.-D are now monotonically decreasing rather than unimodal.

Thus, for perithreshold and suprathreshold feedback, noise simply degrades the SNR. In fact, it degrades the intrinsic reverberatory oscillation, which itself is highly strenghtened by the periodic forcing when the delay and forcing frequency are reciprocally related. As we will see, this is because the intrinsic oscillation is at a frequency close to the reciprocal of the delay (see Section 5), and thus the system exhibits a resonance at this frequency.

4. Parallel network of TCDs with feedback

This ongoing reverberation seen in Figs. 3–5 before and after the signal can interfere with signal detection. Reverberation can be eliminated, all the while significantly increasing the SNR, by using a summing network of parallel feedback loops (Fig. 6) driven by the same periodic signal. In our model, the noise in one loop is uncorrelated with that in other loops, and a given TCD receives feedback only from itself. By analyzing the superposed spike trains from all TCDs, we observe a huge enhancement of the SNR compared to the single-loop case, caused by the cancellation of the uncorrelated firing activity in the summed output. Further, the pre- and post-signal SNR are now drastically lower than during the signal. This summing operation thus allows a clearer separation between the signal and nonsignal conditions.

The effect of the feedback delay τ_D on the SNR is the subject of Fig. 7. At all noise intensities investigated, there are significant resonances at multiples of 0.05 s, the reciprocal of the forcing frequency. Further, at every delay investigated, the succession of SNR values as a function of increasing noise reveals that SR is always present. SR is simply magnified when the reciprocal of the frequency matches an integer multiple of the delay. This matching condition is all the more sharper the larger the delay is (not shown).

These results imply that if a broadband subthreshold signal is presented at the input of this feedback system, its components

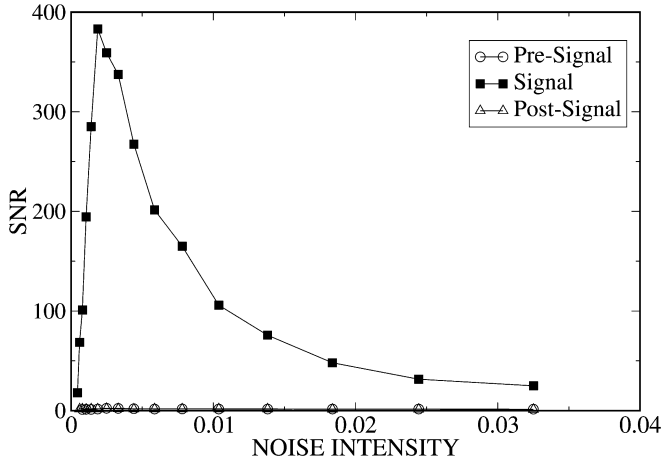

Fig. 6. SNR vs. D for a summing feedback network of 100 parallel detectors in the *subthreshold feedback case* with $G = 0.5$ and $\tau_D = 50$ ms, i.e., the delay equals the value of the forcing period. The output on which the SNR is computed is the sum of the spike trains from each detector. At each noise value, the spike train power spectrum from which the SNR was computed was obtained from an average over 40 realizations of the network dynamics, each realization lasting 1.6 seconds. The different curves are as defined in Fig. 3.

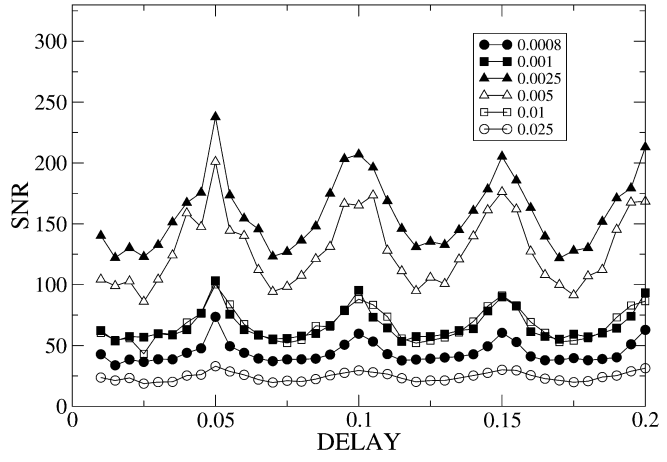

Fig. 7. SNR as a function of the feedback delay for different values of the noise intensity D. Simulations here are for the summing network of 100 detectors in the *subthreshold feedback case* $G = 0.5$, as in Fig. 6. One notices resonances near integer multiples of the delay ($\tau_D = 50$ ms). Further, at each value of the delay used for our simulations, one sees the SNR increase, then decrease, i.e., stochastic resonance is seen at each delay. At each delay and noise intensity, the SNR was determined from an average of 40 realizations of the network dynamics, each lasting 1.6 seconds. The stimulus amplitude was $A = 0.5$, and its frequency was 20 Hz. Since the harmonic structure changes with the delay, the noise floor used for the SNR calculation was estimated as the asymptotic power at high frequency, which is proportional to the mean firing rate.

that match the delay will be strongly amplified and statistically sustained in the loop; in other words, a TCD with delayed feedback can act as a *sharply tuned stochastic resonator*. The origin of these resonances is the subject of the next section.

5. Analysis of the resonances

A full theoretical analysis of these SNR data is not yet possible, due to the nonlinear and non-Markovian nature of these stochastic delayed dynamics, and to the multistability it may exhibit with respect to initial conditions on $(-\tau_D, 0)$ [20]. It is possible however to analyze certain novel dynamical features of this system. To understand the resonant nature of the system in Fig. 1 and its implications for CR and SR, we formulate a dynamical equation for $y(t)$, the voltage input right at the TCD. The basic idea of our approach is to estimate how the amplitude of this voltage depends on the frequency of sinusoidal forcing. It is known [17] for a TCD in open loop that the SNR goes as

$$\mathrm{SNR} = \nu_0 A^2 \Delta_0^2 \sigma^{-4} \exp\bigl[-(\Delta_0/\sigma)^2/2\bigr], \tag{7}$$

where σ is the rms value of the noise. In other words, the SNR depends on the square of the input sinusoidal amplitude. In our system, the amplitude A above will in fact depend on the resonant nature of the TCD with feedback; for example, this amplitude will be replaced by an effective amplitude that will be amplified for certain frequencies. At those frequencies, which as we will see below are near the reciprocals of multiples of the delay, one can expect a larger effective amplitude, and thus expect a higher SNR. In other words, we expect the SNR to reflect the resonance properties of the effective amplitude.

We assume that the lowpass-filtered noise sets the mean TCD threshold-crossing rate according to Eq. (5). However, the barrier height in Eq. (5) is made an instantaneous function of $y(t)$, i.e., $\Delta(t) = \Delta_0 - y(t)$ (see also [17,31] for open-loop situations). We further assume that the time-dependent feedback at the input to the second lowpass filter (Fig. 1(a)) at time t is proportional to the product of the instantaneous threshold crossing rate of the TCD at a time $t - \tau_D$ and the feedback gain. This is simply Campbell's theorem for time-dependent shot noise [32], which allows us to approximate the feedback signal by $g\nu(t - \tau_D)$ (the feedback strength g will be proportional to the feedback gain G used up to now). This assumption is further justified by the fact that, in the absence of feedback, the density of time intervals between successive threshold crossings is very nearly exponential (data not shown)—it is of course exponential for Poisson noise; it remains approximately exponential if the feedback is not too strong. This time-dependent feedback signal is then lowpass-filtered along with the noise and sinusoidal input, yielding

$$\tau \frac{dy}{dt} = -y(t) + A\sin(2\pi f_0 t) + \frac{g}{2\pi\tau\Delta_0} \exp\left\{-\frac{\tau}{D}\bigl[\Delta_0 - y(t-\tau_D)\bigr]^2\right\}. \tag{8}$$

This equation can further be nondimensionalized to

$$\frac{dz}{dt} = -z(t) + \tilde{A}\sin(\tilde{\omega}t) + \frac{g}{2\pi\tau\Delta_0} \exp\left[-\frac{\tau\Delta_0^2}{D}\bigl(1 - z(t-\tilde{\tau}_D)\bigr)^2\right], \tag{9}$$

where time is now in units of the filter time constant τ, $\tilde{\tau}_D \equiv \tau_D/\tau$, $\tilde{\omega} \equiv \omega\tau$, and $\tilde{A} \equiv A/\Delta_0$.

This description only tracks the time-dependent mean of the feedback, which fluctuates with every spike; it neglects the time-dependent variance of this feedback. This variance also increases whenever spikes occur (this can also be understood via

Campbell's theorem), and affects the instantaneous noise intensity at the input to the TCD after the time delay and the response of the second filter. A proper treatment of these fluctuations in the mean and variance, necessary to eventually explain quantitatively the SNR results rather than qualitatively, is beyond the scope of our study. A better approach to that problem is in fact to use global coupling, i.e., to have every TCD feedback to all TCD's, an interesting problem for future work.

We also note that, even without sinusoidal forcing ($A = 0$), there can be more than one fixed point to Eq. (8). Further, bifurcations may occur as parameters are varied. The full study of these possible behavior across parameter space also goes beyond the scope of our study. In particular, an accurate description of the resulting dynamics again requires a proper treatment of how the rate of feedback spikes not only increases the input to the TCD, but also the total noise level.

Here we focus on providing simple analytical insight into the resonant behavior of this system. The sharp tuning of the SNR as a function of delay seen in Fig. 7 for a fixed input frequency can be understood by considering the effect of forcing on Eq. (8) linearized around the fixed point z^*. Defining $Z(t) \equiv z(t) - z^*$, we have

$$\frac{dZ}{dt} = -Z(t) + \beta Z(t - \tilde{\tau}_D) + \tilde{A}\sin(\tilde{\omega}t), \tag{10}$$

where β is the slope of the TCD characteristic at z^*, i.e., $\beta \equiv \frac{df}{dz}(z^*)$ where

$$f\big(z(t)\big) \equiv \frac{g}{2\pi\tau\Delta_0}\exp\left[-\frac{\tau\Delta_0^2}{D}\big(1 - z(t)\big)^2\right]. \tag{11}$$

Without forcing ($A = 0$), the eigenvalues $s = \mu + i\omega$ of this delay-differential equation satisfy $s + 1 - \beta\exp(-s\tilde{\tau}_D) = 0$. Since $\beta > 0$, the infinite number of roots of this equation are all stable. Further, because τ_D/τ is large, the imaginary parts of the eigenvalues are approximately $\omega_i \approx 2\pi k/\tau_D$, $k = 0, \pm1, \pm2, \ldots$. The real parts of these roots are very close to zero, and slowly become more negative with increasing k starting from the value of the most unstable eigenvalue, $s_0 = \mu_0 \approx (\ln\tau)/\tau_D$. This system thus has a real eigenvalue s_0, plus an infinite number of complex conjugate eigenvalues with roughly the same *small* real part but with imaginary parts that are close to harmonics of $\omega_1 \approx 2\pi/\tau_D$. These harmonics can be seen in the spike train spectra in the absence of feedback (not shown), and are reinforced by the presence of periodic forcing near the fundamental of this harmonic structure (see Fig. 2).

The amplitude of the solution of Eq. (10), and by extension of Eq. (8), will then resonate for a driving frequency f_0 close to the inverse of the delay. The stationary solution of Eq. (8) as a function of sinusoidal forcing frequency for different feedback gains is shown in Fig. 8. The resonances are seen at multiples of the reciprocal of the delay. Further, Fig. 9 shows the stationary solution as a function of delay for different feedback gains. The resonance structure is the same as in the simulations of the model system in Fig. 7. It is also seen, in both Figs. 8 and 9, that the resonances are amplified by the feedback gain.

Finally, Fig. 10 shows the amplitude of the oscillations as a function of the delay for different noise intensities (the feedback gain is now constant). One sees the curve move up and then down with increasing noise, which is a manifestation of SR at each individual delay. Near the optimal noise intensity, the resonances are sharper, as they are in the network simulations shown in Fig. 7.

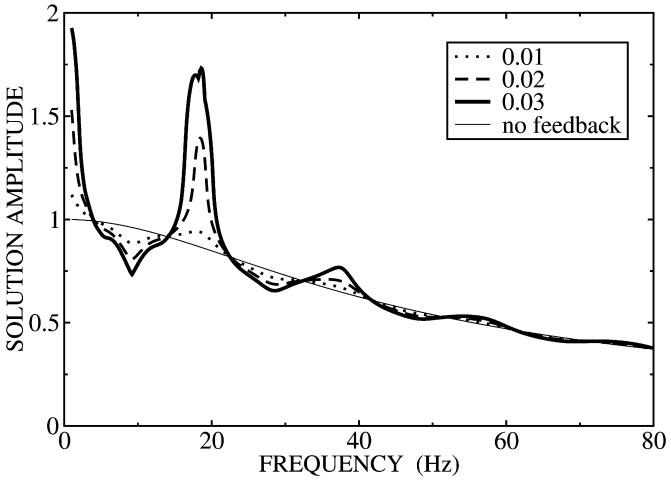

Fig. 8. Steady state amplitude of the solution of Eq. (8) which approximates the behavior of the deterministic rate dynamics, as a function of the sinusoidal stimulus frequency for different values of the feedback strength g. The feedback delay is $\tau_D = 0.05$ s, and the sinusoidal forcing frequency is its reciprocal, 20 Hz. Increasing the feedback strength clearly enhances resonant behavior near integer multiples of an internal mode frequency that is approximately equal to the forcing frequency. Note the monotonically decreasing response in the absence of feedback $g = 0$, illustrating the lowpass open-loop behavior of the system. Numerical integration was carried out using an Euler scheme with time step 0.001 s. Other parameters are $\tau = 0.005$ s, $D = 0.001$, $\Delta_0 = 1.0$, $A = 0.5$ and the initial condition was $x(0) = 0.1$. When $A = 0$, the fixed point was 0.0022, 0.0045 and 0.0069 for $g = 0.01$, 0.02 and 0.03, respectively.

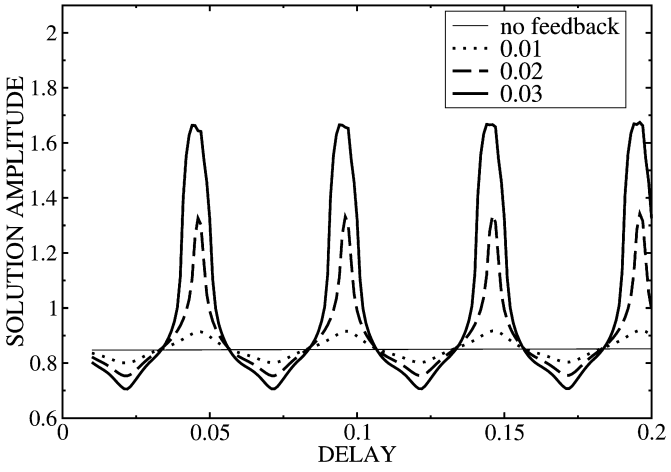

Fig. 9. Steady state amplitude of the solution of Eq. (8) which approximates the behavior of the deterministic rate dynamics, as a function of the feedback delay for different values of the feedback strength g. The sinusoidal forcing frequency is equal to 20 Hz. As in this figure, increasing the feedback strength clearly enhances resonant behavior near integer multiples of the delay. Note the flat response in the absence of feedback ($g = 0$). Parameters are as in Fig. 8.

Since it is known that the SNR for the usual open-loop TCD increases with the square of the amplitude of the periodic forcing as in Eq. (7), the resulting large amplitude motion in Eq. (8) in response to the resonant forcing will also increase the SNR

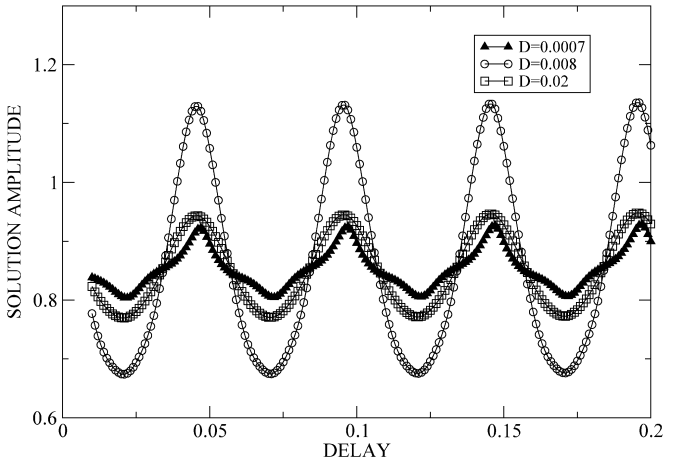

Fig. 10. Steady state amplitude of the solution of Eq. (8) which approximates the behavior of the deterministic rate dynamics, as a function of the feedback delay for different values of the noise intensity D. The sinusoidal forcing frequency is equal to 20 Hz. The curves first increase, then decrease as a function of noise intensity, as in Fig. 7. Parameters are as in Fig. 8, and the gain was set at $g = 0.02$.

in closed loop. Further, since such motion in the full nonlinear system Eq. (8) will generate, by mode-coupling, power at harmonics of the forcing period, and since the other resonant modes of the linearized system are close to these harmonics, resonances will occur at these harmonics as well.

The negative feedback dynamics [33] are likely to also display coherence resonance and stochastic resonance, to include bifurcations to oscillatory behavior, and to exhibit resonances at harmonics of π/τ_D. This, along with combinations of positive and negative feedback, as occur in many applications, will be presented elsewhere. The highly complex dynamics of a simple TCD with delayed feedback are clearly not of the "non-dynamical" type, as in the open-loop case. The specific interplay of their deterministic and stochastic resonance properties will depend on the particular shape of the input–output characteristic of the TCD, including the usual presence of a refractory period, in the particular physical, chemical or biological context.

Acknowledgements

This work was funded by Defeating Deafness (R.M.) and NSERC Canada (A.L.).

References

[1] J. Bechhoefer, Rev. Mod. Phys. 77 (2005) 783.
[2] K. Ikeda, K. Kondo, O. Akimoto, Phys. Rev. Lett. 49 (1982) 1467; S. Lepri, et al., Physica D 70 (1993) 235.
[3] G.D. Van Wiggeren, R. Roy, Science 279 (1998) 1198; H.D.I. Abarbanel, M.B. Kennel, Phys. Rev. Lett. 80 (1998) 3153.
[4] J.E.S. Socolar, D.W. Sukow, D.J. Gauthier, Phys. Rev. E 50 (1994) 3245; J.M. Buldu, J. Garcia-Ojalvo, M.C. Torrent, Phys. Rev. E 69 (2004) 046207.
[5] I.R. Epstein, Int. Rev. Phys. Chem. 11 (1992) 135; T. Chevalier, A. Freund, J. Ross, J. Chem. Phys. 95 (1991) 308.
[6] K. Pakdaman, et al., Neural Networks 9 (1996) 797; O. Diez Martinez, J.P. Segundo, Biol. Cybern. 47 (1983) 33.
[7] W. Gerstner, Phys. Rev. Lett. 76 (1996) 1755; P.C. Bressloff, S. Coombes, Physica D 126 (1999) 99; R.E. Plant, SIAM J. Appl. Math. 40 (1981) 150.
[8] C.M. Marcus, R.M. Westerwelt, Phys. Rev. A 39 (1989) 347; A.V.M. Herz, Z. Li, J.L. van Hemmen, Phys. Rev. Lett. 66 (1991) 1370; J. Belair, J. Dynamics Differential Equations 5 (1993) 607; D. Hansel, H. Sompolinsky, Phys. Rev. Lett. 68 (1992) 718.
[9] L. Glass, M.C. Mackey, From Clocks to Chaos: The Rhythms of Life, Princeton Univ. Press, Princeton, 1988.
[10] L. Glass, C.P. Malta, J. Theor. Biol. 145 (1990) 217; M. Courtemanche, L. Glass, J.P. Keener, Phys. Rev. Lett. 70 (1993) 2182.
[11] K. Pyragas, Phys. Lett. A 170 (1992) 421; T. Aida, P. Davis, IEEE J. Quantum Electron. 28 (1992) 686; B. Mensour, A. Longtin, Phys. Lett. A 205 (1995) 18; Y. Zhang, et al., Phys. Rev. E 57 (1998) 1611.
[12] H.U. Voss, Phys. Rev. Lett. 87 (2001) 014102; C. Masoller, Phys. Rev. Lett. 88 (2002) 034102.
[13] A. Longtin, et al., Phys. Rev. A 41 (1990) 6992; Y. Chen, M. Ding, J.A.S. Kelso, Phys. Rev. Lett. 79 (1997) 4501; J.L. Cabrera, J.G. Milton, Phys. Rev. Lett. 89 (2002) 157802; D. Huber, L.S. Tsimring, Phys. Rev. E (2005), in press.
[14] L. Gammaitoni, et al., Rev. Mod. Phys. 70 (1998) 223.
[15] A. Pikovsky, J. Kurths, Phys. Rev. Lett. 78 (1997) 775.
[16] P. Jung, Phys. Rev. E 50 (1994) 2513.
[17] Z. Gingl, L.B. Kiss, F. Moss, Nuovo Cimento D 17 (1995) 795; X. Pei, L. Wilkens, F. Moss, Phys. Rev. Lett. 77 (1996) 4679.
[18] X. Godivier, F. Chapeau-Blondeau, Europhys. Lett. 35 (1996) 473.
[19] L. Gammaitoni, Phys. Rev. E 52 (1995) 4691; N. Stocks, Phys. Rev. Lett. 84 (2000) 2310.
[20] J. Foss, et al., Phys. Rev. Lett. 76 (1996) 708; J. Foss, J. Milton, F. Moss, Phys. Rev. E 55 (1996) 4536.
[21] S. Kim, S.H. Park, H.-B. Pyo, Phys. Rev. Lett. 82 (1999) 1620.
[22] T. Ohira, Y. Sato, Phys. Rev. Lett. 82 (1999) 2811.
[23] T. Prager, L. Schimansky-Geier, Phys. Rev. Lett. 91 (2003) 230601.
[24] N.B. Janson, A.G. Balanov, E. Schöll, Phys. Rev. Lett. 93 (2004) 010601.
[25] C.C. Chow, T.T. Imhoff, J.J. Collins, Chaos 8 (1998) 616.
[26] L. Gammaitoni, et al., Phys. Rev. Lett. 82 (1999) 4574.
[27] L. Tsimring, A. Pikovsky, Phys. Rev. Lett. 87 (2001) 250602; A. Krawiecki, T. Stemler, Phys. Rev. E 68 (2003) 061101.
[28] P. Jung, et al., New J. Phys. 7 (2005) 17.
[29] S.O. Rice, Bell Syst. Tech. J. 23 (1944) 282; S.O. Rice, Bell Syst. Tech. J. 24 (1945) 46.
[30] A.R. Bulsara, et al., Phys. Rev. E 53 (1995) 3958; T. Shimokawa, et al., Phys. Rev. E 59 (1999) 3461.
[31] R.P. Morse, E.F. Evans, Nature Med. 2 (1996) 928; R.P. Morse, P. Roper, Phys. Rev. E 61 (2000) 5683.
[32] A. Papoulis, Probability, Random Variables, and Stochastic Processes, third ed., McGraw–Hill, New York, 1991.
[33] S.N. Chow, J. Mallet-Paret, in: J. Chandra, A.C. Scott (Eds.), Coupled Nonlinear Oscillators, North-Holland, Amsterdam, 1983, pp. 7–12.